



RESEARCH ARTICLE OPEN ACCESS

TRAF7-Mutated Fibromyxoid Spindle Cell Tumor of Bone: An Osseous Case Expanding the Spectrum of TRAF7-Mutated Tumors With Over 20 Years Clinical Follow-Up

Laura M. Warmke¹  | Ani Toklu¹ | Spencer M. Richardson² | Christopher D. Collier² | L. Daniel Wurtz²  | Lauren M. Ladd³ | Roman Shrestha³ | Devin J. Conway²

¹Department of Pathology and Laboratory Medicine, Indiana University School of Medicine, Indianapolis, Indiana, USA | ²Department of Orthopedic Surgery, Indiana University School of Medicine, Indianapolis, Indiana, USA | ³Department of Radiology and Imaging Sciences, Indiana University School of Medicine, Indianapolis, Indiana, USA

Correspondence: Laura M. Warmke (lwarmke@iu.edu)

Received: 24 January 2026 | **Revised:** 25 February 2026 | **Accepted:** 5 March 2026

Keywords: fibromyxoid | L1CAM | mesenchymal neoplasm | sarcoma | TRAF7

ABSTRACT

TRAF7 mutations are a rare occurrence in human cancer and have recently been described in a group of mesenchymal tumors with varying clinical course. Herein, we expand the spectrum of *TRAF7*-mutated fibromyxoid spindle cell tumors by reporting the first case to arise in bone. A 60-year-old woman presented with right knee pain and was incidentally found to have a left distal femur lesion, which was first detected 20 years prior when it was favored to be benign. Recent imaging studies revealed significant interval growth with focal cortical destruction and soft tissue extension. Histologic examination showed a bland spindle cell neoplasm with fibrous to myxoid stroma. Rare mitotic figures were present; necrosis and marked cytologic atypia were absent. Immunohistochemical work-up showed that the spindle cells only demonstrated focal cytoplasmic staining with L1CAM, and whole exome sequencing identified a *TRAF7* p.Y563C missense mutation. The tumor was resected, and the patient is recovering well at 2 months with no evidence of local recurrence or distant disease. This report is the first known case of a *TRAF7*-mutated fibromyxoid spindle cell tumor of bone with the longest clinical follow-up reported to date.

1 | Introduction

TRAF7 mutations are a rare occurrence in human cancer with an overall frequency of <7% [1]. Higher frequencies of somatic *TRAF7* mutations have been identified in meningioma (23%–29%) [2], especially the secretory (97%) [3] and chordoid (27%) [4] subtypes, intraneural perineurioma (63%) [5], adenomatoid tumor of genital type (85%) [6–8], malignant pleural mesothelioma (~2%) [9], localized pleural mesothelioma (33%) [10], and well-differentiated papillary peritoneal mesothelioma (90%) [11–13]. In contrast, germline mutations in *TRAF7* have been

detected in patients with developmental delay and cardiofacial defects [14, 15].

The TRAF7 protein is part of the tumor necrosis factor (TNF) receptor-associated factor (TRAF) family of intracellular proteins. TRAF7 is one of seven known mammalian TRAF proteins (TRAF1–7) and is known to interact with MEKK3 and regulate the nuclear factor-kappa B (NF- κ B) signaling pathway [5]. All the TRAF proteins, except for TRAF1, have a RING finger domain localized at their N-terminus, which possesses E3 ubiquitin ligase activity, followed by one or more zinc finger domains

This is an open access article under the terms of the [Creative Commons Attribution](https://creativecommons.org/licenses/by/4.0/) License, which permits use, distribution and reproduction in any medium, provided the original work is properly cited.

© 2026 The Author(s). Genes, Chromosomes and Cancer published by Wiley Periodicals LLC.

[16]. Unique to this group, the C-terminus of TRAF7 contains seven WD40 repeats [17], composed of repeating units of 40–60 variable residues that end in tryptophan (W) and aspartate (D) dipeptides. Somatic *TRAF7* mutations in tumors typically occur in this C-terminal hotspot region of WD40 repeats, which leads to activation of the NF- κ B signaling pathway.

In 2023, Dermawan et al. reported three cases of *TRAF7*-mutated fibromyxoid spindle cell tumor arising in the deep soft tissue of adult patients with aggressive clinical behavior despite a low-grade histologic appearance [18]. Shortly thereafter, in 2025, a fourth case of *TRAF7*-mutated myxoid and spindle cell mesenchymal tumor involving both soft tissue and bowel was reported in an immunocompromised pediatric patient [19]. Herein, we report the first known case of a *TRAF7*-mutated fibromyxoid spindle cell tumor of bone with over 20 years clinical follow-up, thereby expanding the clinicopathologic spectrum of this rare and emerging mesenchymal neoplasm.

2 | Materials and Methods

2.1 | Case Selection

This study was approved by the Institutional Review Board of Indiana University (protocol #17625). The case was identified through routine clinical practice, and the clinicopathologic features were assessed by the authors.

2.2 | Immunohistochemistry

A panel of immunohistochemical stains was performed on 4- μ m formalin-fixed paraffin-embedded (FFPE) tissue sections

using standard techniques. Detection and staining were performed using a fully automated DAB antigen retrieval system (Benchmark ULTRA; Ventana Medical Systems, Tucson, AZ, USA), with appropriate controls. The following antibodies were used: mouse monoclonal anti-L1CAM (UJ127.11, RTU; Sigma-Aldrich, St. Louis, MO), mouse monoclonal anti-cytokeratin (AE1/AE3, RTU; Dako, Santa Clara, CA), rabbit polyclonal anti-S100 protein (RTU; Dako, Santa Clara, CA), mouse monoclonal anti-SMA (1A4, RTU; Dako, Santa Clara, CA), mouse monoclonal anti-beta-catenin (14, RTU; Cell Marque, Rocklin, CA), mouse monoclonal anti-desmin (D33, RTU; Dako, Santa Clara, CA), mouse monoclonal anti-CD34 (QBEnd10, RTU; Dako, Santa Clara, CA), mouse monoclonal anti-EMA (E29, RTU; Dako, Santa Clara, CA), mouse monoclonal anti-MUC4 (8G7, RTU; Cell Marque, Rocklin, CA), and rabbit monoclonal anti-GRM1 (JM11-61, 1:500; Thermo Fisher Scientific Inc., Waltham, MA). The immunohistochemical stain for GRM1 and interpretation was performed at Stanford Anatomic Pathology and Clinical Laboratories. The threshold for designating positivity was expression in > 5% of cells.

2.3 | Fluorescence in Situ Hybridization (FISH)

Fluorescence in situ hybridization for *MDM2* (12q15) amplification was performed at Mayo Clinic Laboratories according to previously described protocols [20].

2.4 | Next-Generation Sequencing (NGS)

Next-generation sequencing was performed through Caris Life Sciences. Whole exome sequencing with a high-throughput assay analyzed over 22000 DNA genes, and a 250000 evenly

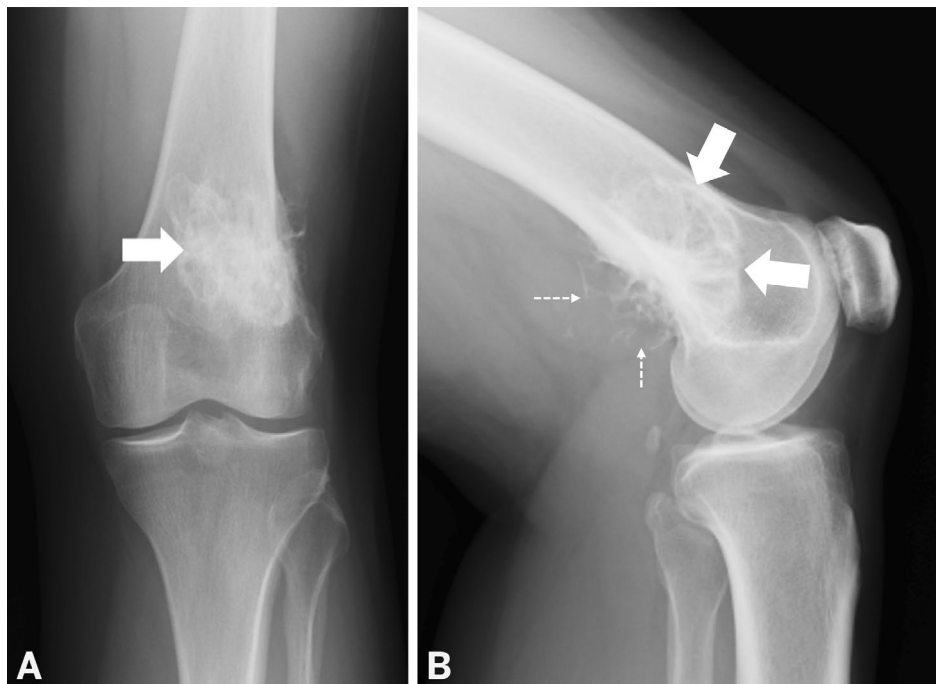


FIGURE 1 | Radiograph. AP (A) and lateral (B) radiographs of the left knee show a large, partially sclerotic intraosseous and extraosseous lesion in the distal femoral metaphysis (wide arrows), centered at the posterolateral cortex with irregular central internal mineralization of the posterior extraosseous component (dashed arrow).

spaced genome single nucleotide polymorphism back-bone was used to enhance detection of genome-level alterations.

3 | Results

3.1 | Clinical Summary and Radiologic Findings

A 60-year-old woman with a medical history of osteoporosis treated with alendronate and a surgical history of a right anterior cruciate ligament reconstruction 30 years ago presented with right knee pain after tripping over her dog. Imaging work-up revealed no acute pathology in her right knee but incidentally noted a left distal femur lesion. She reported that the left femur lesion had first been detected 20 years ago, when it was small and favored to be benign.

Dedicated radiographs of her left knee showed an irregular, partly sclerotic lesion centered at the posterolateral cortex of her distal femoral metaphysis with intraosseous and extraosseous components, a thick posterior periosteal reaction, and reticular mineralization of the extraosseous soft tissue mass (Figure 1). Follow-up MRI of her left knee showed a T1-hypointense,

T2-hyperintense mass (6.0cm) in the posterior distal femoral metaphysis with intramedullary and extraosseous extension (Figure 2A–D). Focal cortical destruction was present, though peripheral sclerosis about the intramedullary component and thick periosteal reaction deep to the extraosseous component suggested a slow-growing process. Internal hypointense septations, corresponding to internal calcification, were present with heterogeneous mild internal enhancement, primarily at the periphery and in the internal septations. Review of the initial CT imaging 20 years prior showed a much smaller exophytic, cortically based lesion with saucerization and sclerosis of the cortex and a hypodense soft tissue mass with thin, ring-and-arc-type central mineralization (Figure 2E,F), suggestive of a surface bone lesion and favored to represent a juxtacortical chondroma at that time. The patient was subsequently lost to follow-up until the lesion was incidentally rediscovered.

3.2 | Gross, Histopathologic, and Immunohistochemical Findings

Biopsy of the lesion showed a low-grade-appearing spindle cell neoplasm with fibrous and myxoid stroma (Figure 3A,B). No

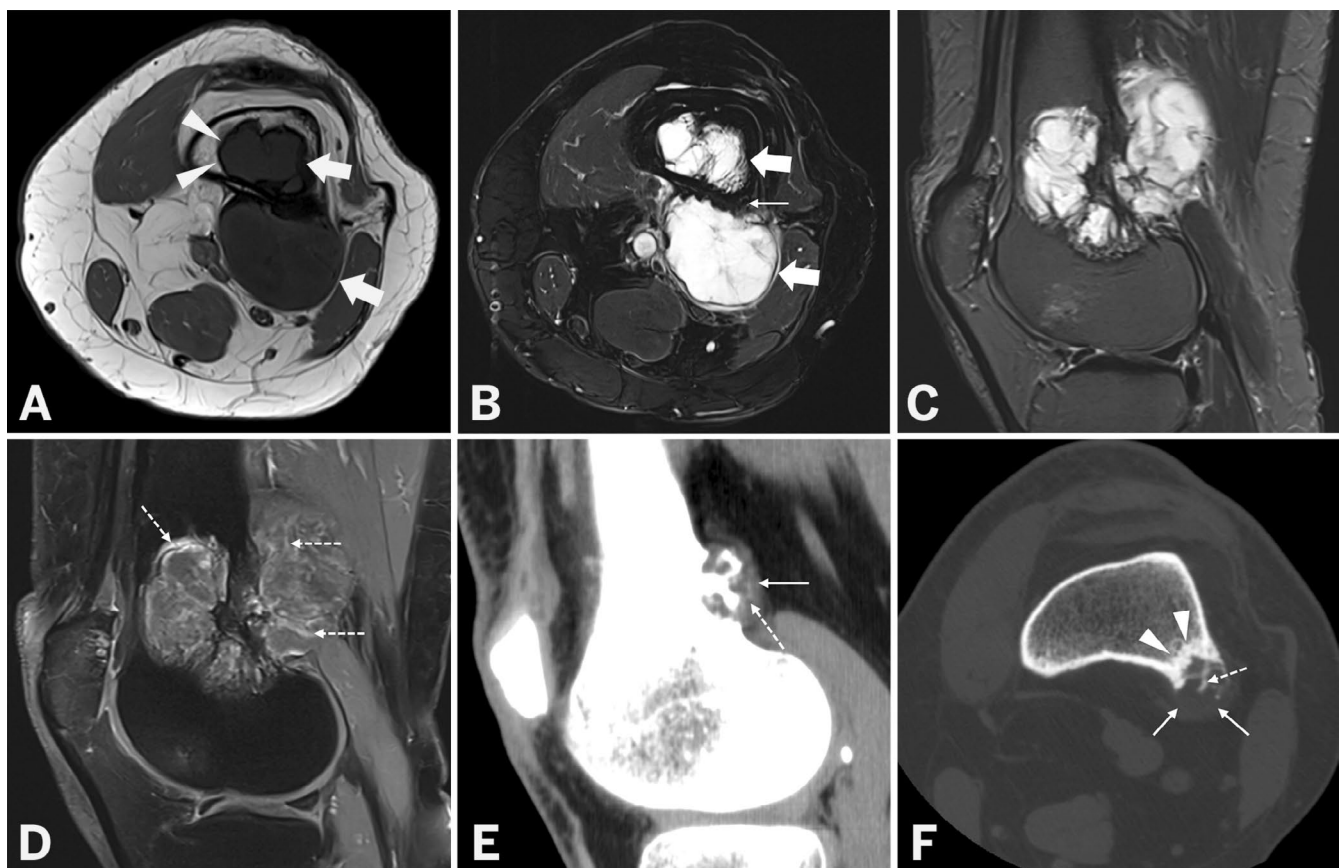


FIGURE 2 | Current MRI and CT from 20 years prior. MR imaging (A, axial T1; B, axial T2 FS) shows a large T1-hypointense, T2-hyperintense mass (thick arrows) in the posterior distal femoral metaphysis with intramedullary and extraosseous components. Peripheral sclerosis (arrowheads) and a thick periosteal reaction are present (thin arrow). Sagittal MR images (C, sagittal MODIR; D, sagittal T1 FS + C) again show the large, lobulated mass with focal cortical destruction and heterogeneous mild internal enhancement, primarily at the periphery and internal septations (dashed arrows). CT images (E, sagittal; F, axial) from 20 years prior show a cortically based exophytic lesion at the posterolateral distal femoral metaphysis with saucerization and sclerosis of the cortex (arrowheads) and a hypodense soft tissue mass (thin arrow) with the appearance of thin, ring-and-arc mineralization centrally (dashed arrow).

tumor necrosis and no marked cytologic atypia or pleomorphism were identified. Rare mitotic figures (up to 3 per 10 high-powered fields) without atypical forms were present.

An immunohistochemical stain for L1CAM demonstrated cytoplasmic staining in approximately 30% of the lesional cells (Figure 3G); CK AE1/AE3, S100 protein, SMA, beta-catenin, desmin, CD34 (Figure 3H), EMA (Figure 3I), MUC4, and GRM1 were essentially negative. All control slides stained appropriately.

Subsequent resection showed a well-defined, solid, and multi-lobulated mass involving bone with focal cortical destruction and soft tissue extension (Figure 4). Dense, tan-white fibrous areas were present along with prominent myxoid areas. The histology of the resection was essentially identical to the biopsy, showing focal areas with increased cellularity and a more

epithelioid appearance (Figure 3C-F). The tumor was relatively circumscribed but unencapsulated, with focal infiltration into the surrounding adipose tissue.

3.3 | Cytogenetic and Molecular Findings

Fluorescence in situ hybridization (FISH) for *MDM2* amplification was negative. Whole exome sequencing detected a somatic pathogenic alteration in the *TRAF7* gene (c. 1688 A>G). The missense mutation (*TRAF7* p.Y563C) was in the C-terminal WD40 repeat domain of the encoded TRAF7 protein (Figure 5). The variant allele frequency was 19%, and the depth of coverage was 1144. No other pathogenic alterations, mutations, or significant copy number alterations were identified. Microsatellite instability (MSI) was stable. Both tumor mutational burden (2 mut/Mb) and genomic loss of heterozygosity (7%) were low.

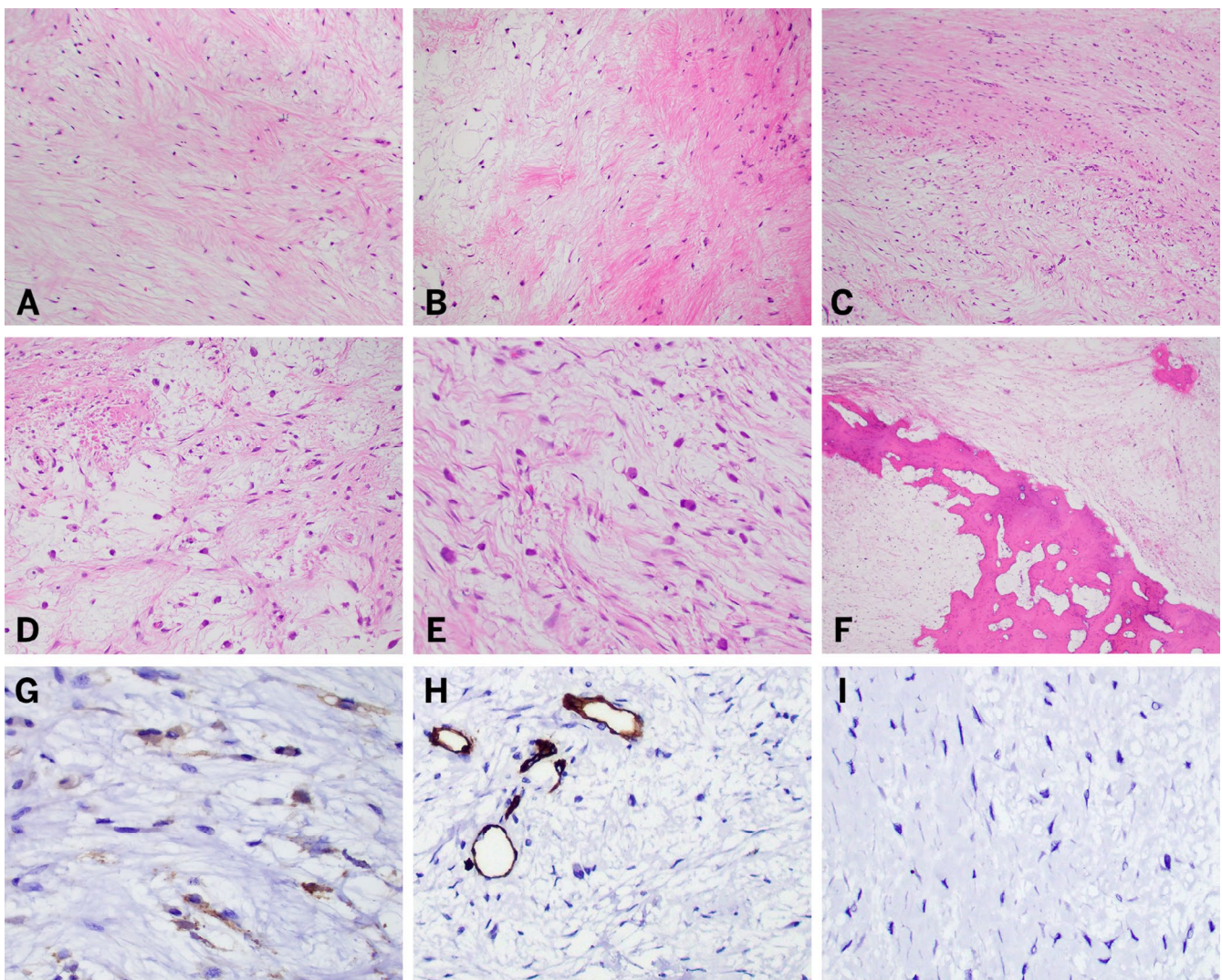


FIGURE 3 | Histologic and immunohistochemical findings. The biopsy showed a low-grade-appearing spindle cell neoplasm (A) with fibrous and myxoid stroma (B). The resection showed similar findings with areas of increased cellularity reminiscent of LGFMS (C). Focal areas showed tumor cells with a more epithelioid appearance and mild to moderate cytologic atypia (D, E). Infiltration of bone (F) with soft tissue extension was present. Immunohistochemical stains showed that the lesional cells demonstrated focal cytoplasmic staining with L1CAM (G), while they were essentially negative for CD34 (H) and EMA (I).

3.4 | Clinical Follow-Up

Prior to resection, PET scan showed mild hypermetabolism of the left distal femoral mass (max SUV 3.7) without evidence of distant metastasis. At present, the patient is recovering well from distal femoral resection with hinged knee replacement and undergoing active surveillance with no evidence of disease at 2 months post resection.

4 | Discussion

To date, including our case, only five cases of *TRAF7*-mutated fibromyxoid spindle cell tumor have been reported (Table 1). In 2023, Dermawan et al. reported three cases of deep soft tissue lesions arising in adult patients [18]. The tumors occurred in two women and one man with an age range of 63–75 years (median: 67 years). The masses involved the shoulder, chest wall, and thigh. Tumor size ranged from 7.0 to 9.1 cm in greatest dimension (median: 7.8 cm). Despite a low-grade histologic appearance, two patients developed distant metastatic disease, involving the lungs and bone, and both died of disease at 5 and 36 months. The metastatic lesions were noted to have increased mitotic activity and a more epithelioid appearance without necrosis. The third patient was alive with no evidence of disease at 9 months. In 2025, Torres et al. reported the fourth

and first pediatric case, a large abdominopelvic mass arising in a 13-year-old girl with a history of heart and renal transplant [19]. The possible connection to immunosuppression in this case mirrors the suggested association between immunosuppression and adenomatoid tumors with *TRAF7* mutations [7, 8]. Following resection, the young girl is stable and on active surveillance at 7 months. Compared to these four prior cases, the present case represents the first confirmed bone primary with the longest clinical follow-up reported to date, expanding the clinicopathologic spectrum of this rare and emerging mesenchymal neoplasm.

The location of this lesion, arising on the cortical surface of the posterior aspect of the distal femur, raised the possibility of a parosteal osteosarcoma. The patient's prolonged clinical history and presence of intramedullary extension support the diagnosis; however, parosteal osteosarcoma demonstrates considerably higher prevalence among young adults, with its peak incidence during the third decade of life. While the current case does demonstrate a low-grade spindle cell appearance, the parallel and well-formed fascicles of woven bone, characteristic of parosteal osteosarcoma, are missing. Furthermore, FISH for *MDM2* amplification, which is present in the majority of parosteal osteosarcoma, was also negative. Given the fibromyxoid appearance of the lesion, a chondromyxoid fibroma (CMF) was also considered. CMF is a benign cartilaginous neoplasm characteristically composed of stellate or spindle-shaped cells in a myxoid to fibrous background. The distal femur is a common site for CMF, and evidence of cortical destruction may be seen. On a molecular level, most CMFs show rather specific upregulation of *GRM1* expression. Unlike CMF, which typically shows immunohistochemical expression of both *GRM1* and *S100* protein, this lesion was negative for both markers, and the tumor further showed uncharacteristically aggressive features on imaging. Another fibromyxoid lesion in the differential diagnosis is a low-grade fibromyxoid sarcoma (LGFMS). LGFMS typically contains bland spindle cells with alternating collagenous and myxoid areas. While LGFMS much more typically arises in soft tissue, rare cases occurring in bone have been reported [21]. The majority (>90%) of LGFMS have *FUS::CREB3L2* gene fusions and demonstrate strong immunohistochemical expression of *MUC4*, both of which were missing in this case. Given the presence of a *TRAF7* mutation, a perineurioma was briefly considered. Arguing against perineurioma, this case lacked a whorled to lamellar architecture and immunohistochemical expression of EMA, both features typically seen in perineurioma. Like

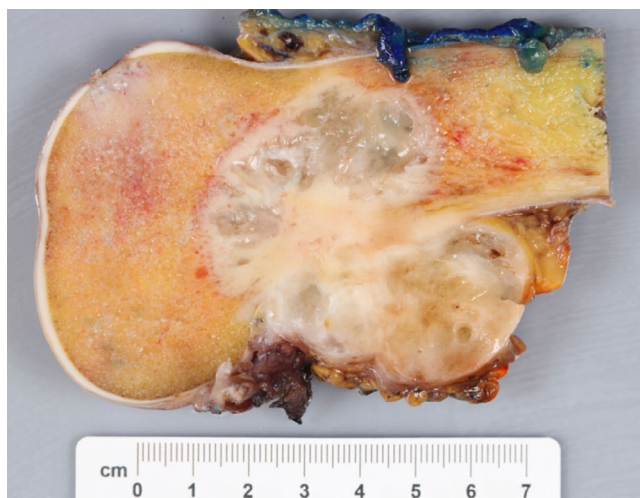


FIGURE 4 | Gross pathology of resection. The resection showed a well-defined, solid, and multilobulated mass involving bone with focal cortical destruction and soft tissue extension.



FIGURE 5 | *TRAF7* protein with mutation. The *TRAF7* protein has a RING finger domain localized at its N-terminus, which has E3 ubiquitin ligase activity, and is followed by a zinc finger domain. The C-terminus contains seven WD40 repeats, and the missense mutation p.Y563C (arrowhead) occurs in this hotspot region. The corresponding amino acid positions (Pos.) are indicated at the bottom of the figure.

TABLE 1 | *TRAF7*-mutated fibromyxoid spindle cell tumors of bone and soft tissue.

Case	Age (year)/Sex	Site	Size (cm)	Mitotic activity	Necrosis	IHC (+)	IHC (-)	<i>TRAF7</i> mutation (VAF%)	Clinical follow-up (mo post resection)	References
1	67/M	Shoulder	7.8	10 per 10 hpf in metastasis	Absent	SMA	Keratin, S100 protein, desmin, Melan-A, beta-catenin, MUC4, CD34, STAT6	p.P398S (6.1%), p.Y577S (8.0%)	DOD (36) with distant metastasis	[18]
2	63/F	Chest wall	7.0	No significant mitotic activity	Absent	SMA (focal), CD34, GLUT1	S100 protein, SOX10, desmin, beta-catenin, MUC4, STAT6, EMA, pan-TRK, ALK, ER	p.G536S (21.5%)	ANED (9)	[18]
3	75/F	Thigh	9.1	No significant mitotic activity	Absent	CD34, WT1, PR, MDM2 (scattered)	Keratin, SMA, desmin, CD1a, CD163, CD68, calretinin, PAX8, ALK, CDK4	p.N632K (14.2%)	DOD (5) with distant metastasis	[18]
4	13/F	Abdomen/ Pelvis	12.6	13 per 10 hpf	Absent	CD34	CAM5.2, S100 protein, SOX10, SMA, desmin, D2-40, GLUT1	p.S561R (44%)	ANED (7)	[19]
5	60/F	Femur	6.0	3 per 10 hpf	Absent	L1CAM	CK AE1/AE3, S100 protein, SMA, beta-catenin, desmin, CD34, EMA, MUC4, GRM1	p.Y563C (19%)	ANED (2)	Current case

Abbreviations: ANED, alive no evidence of disease; DOD, died of disease; F, female; hpf, high-powered fields; IHC, immunohistochemistry; M, male; mo, months; VAF, variant allele frequency; y, years.

perineurioma, meningioma is also well known to have *TRAF7* mutations. In contrast to this lesion, meningiomas characteristically arise in intracranial locations. While meningiomas can invade bone, and rarely occur outside the neuraxis, a primary lesion involving the distal femur would be very unusual.

A comprehensive immunohistochemical work-up revealed that our case only demonstrated focal cytoplasmic staining with L1 cell adhesion molecule (L1CAM). L1CAM is a known transcriptional target of NF- κ B and has emerged as a reliable surrogate marker for tumors with activated NF- κ B signaling [22, 23]. A previous study by Goode et al. showed that mutant but not wildtype *TRAF7* led to increased phosphorylation of NF- κ B, a modification that leads to activation and upregulation of L1CAM expression, a downstream transcriptional target of NF- κ B [7]. Immunohistochemical expression of L1CAM, ranging from focal to robust, has been reported in other tumors with *TRAF7* mutations, including adenomatoid tumor [7] and well-differentiated papillary mesothelioma [13]. While molecular confirmation remains the gold standard, immunohistochemical expression of L1CAM may be useful as a surrogate marker for activating *TRAF7* mutations and as a screening tool for these rare mesenchymal neoplasms.

Molecular studies revealed that the *TRAF7* mutation was the sole significant alteration, indicating that it is likely the driver of pathogenesis. Like other tumors with *TRAF7* mutations, the missense mutation occurred in the C-terminal hotspot WD40 repeat region. While the specific *TRAF7* p.Y563 mutation found in this case has previously been reported in both meningioma and mesothelioma [16, 24], this case fit best with the previously described *TRAF7*-mutated fibromyxoid spindle cell tumors [18, 19]. Methylation studies had shown that these mesenchymal neoplasms clustered closest to the undifferentiated sarcoma and myxofibrosarcoma methylation classes [18]; however, their clinical, molecular, and methylation profiles suggest that they most likely represent a distinct entity. The limited cases reported to date have shown a spectrum of clinicopathologic behavior. While two deep soft tissue lesions have demonstrated a highly aggressive clinical course, despite low-grade-appearing histology, this case, along with the only reported pediatric case, has shown much more indolent behavior. Overall, the clinical behavior of *TRAF7*-mutated mesenchymal tumors remains uncertain, and more data is needed to fully understand these rare tumors. Given the possibility of aggressive behavior, complete resection with active surveillance is recommended.

Acknowledgments

The authors thank the talented illustrator and graphic designer Fredrik Skarstedt for his help and Dr. Gregory W. Charville for his expertise with GRM1 immunohistochemistry.

Funding

The authors have nothing to report.

Conflicts of Interest

The authors declare no conflicts of interest.

Data Availability Statement

The data that support the findings of this study are available from the corresponding author upon reasonable request.

References

1. S. Zhu, J. Jin, S. Gokhale, et al., "Genetic Alterations of TRAF Proteins in Human Cancers," *Frontiers in Immunology* 9 (2018): 2111.
2. V. E. Clark, E. Z. Erson-Omay, A. Serin, et al., "Genomic Analysis of Non-NF2 Meningiomas Reveals Mutations in *TRAF7*, *KLF4*, *AKT1*, and *SMO*," *Science* 339, no. 6123 (2013): 1077–1080.
3. D. E. Reuss, R. M. Piro, D. T. Jones, et al., "Secretory Meningiomas Are Defined by Combined *KLF4* K409Q and *TRAF7* Mutations," *Acta Neuropathologica* 125, no. 3 (2013): 351–358.
4. M. M. Georgescu, A. Nanda, Y. Li, et al., "Mutation Status and Epithelial Differentiation Stratify Recurrence Risk in Chordoid Meningioma-A Multicenter Study With High Prognostic Relevance," *Cancers* 12, no. 1 (2020): 225.
5. C. J. Klein, Y. Wu, M. E. Jentoft, et al., "Genomic Analysis Reveals Frequent *TRAF7* Mutations in Intraneural Perineuriomas," *Annals of Neurology* 81, no. 2 (2017): 316–321.
6. H. Itami, T. Fujii, T. Nakai, et al., "*TRAF7* Mutations and Immunohistochemical Study of Uterine Adenomatoid Tumor Compared With Malignant Mesothelioma," *Human Pathology* 111 (2021): 59–66.
7. B. Goode, N. M. Joseph, M. Stevers, et al., "Adenomatoid Tumors of the Male and Female Genital Tract Are Defined by *TRAF7* Mutations That Drive Aberrant NF- κ B Pathway Activation," *Modern Pathology* 31, no. 4 (2018): 660–673.
8. D. Tamura, D. Maeda, S. A. Halimi, et al., "Adenomatoid Tumour of the Uterus Is Frequently Associated With Iatrogenic Immunosuppression," *Histopathology* 73, no. 6 (2018): 1013–1022.
9. R. Bueno, E. W. Stawiski, L. D. Goldstein, et al., "Comprehensive Genomic Analysis of Malignant Pleural Mesothelioma Identifies Recurrent Mutations, Gene Fusions and Splicing Alterations," *Nature Genetics* 48, no. 4 (2016): 407–416.
10. Y. P. Hung, F. Dong, A. M. Dubuc, P. Dal Cin, R. Bueno, and L. R. Chirieac, "Molecular Characterization of Localized Pleural Mesothelioma," *Modern Pathology* 33, no. 2 (2020): 271–280.
11. W. Yu, W. Chan-On, M. Teo, et al., "First Somatic Mutation of *E2F1* in a Critical DNA Binding Residue Discovered in Well-Differentiated Papillary Mesothelioma of the Peritoneum," *Genome Biology* 12, no. 9 (2011): R96.
12. M. Offin, N. Aguirre, S. R. Yang, et al., "Clinical Characteristics and Outcomes of Patients With Well-Differentiated Papillary Peritoneal Mesothelial Tumors," *Annals of Surgical Oncology* 31, no. 12 (2024): 7973–7977.
13. M. Stevers, J. T. Rabban, K. Garg, et al., "Well-Differentiated Papillary Mesothelioma of the Peritoneum Is Genetically Defined by Mutually Exclusive Mutations in *TRAF7* and *CDC42*," *Modern Pathology* 32, no. 1 (2019): 88–99.
14. M. J. Tokita, C. A. Chen, D. Chitayat, et al., "De Novo Missense Variants in *TRAF7* Cause Developmental Delay, Congenital Anomalies, and Dysmorphic Features," *American Journal of Human Genetics* 103, no. 1 (2018): 154–162.
15. L. Castilla-Vallmanya, K. K. Selmer, C. Dimartino, et al., "Phenotypic Spectrum and Transcriptomic Profile Associated With Germline Variants in *TRAF7*," *Genetics in Medicine* 22, no. 7 (2020): 1215–1226.
16. T. Zotti, I. Scudiero, P. Vito, and R. Stilo, "The Emerging Role of *TRAF7* in Tumor Development," *Journal of Cellular Physiology* 232, no. 6 (2017): 1233–1238.

17. T. Zotti, P. Vito, and R. Stilo, "The Seventh Ring: Exploring TRAF7 Functions," *Journal of Cellular Physiology* 227, no. 3 (2012): 1280–1284.
18. J. K. Dermawan, L. Villafania, T. Bale, et al., "TRAF7-Mutated Fibromyxoid Spindle Cell Tumors Are Associated With an Aggressive Clinical Course and Harbor an Undifferentiated Sarcoma Methylation Signature: A Molecular and Clinicopathologic Study of 3 Cases," *American Journal of Surgical Pathology* 47, no. 2 (2023): 270–277.
19. S. Torres, Z. High, Q. Wang, et al., "TRAF7-Mutated Myxoid and Spindle Cell Mesenchymal Tumor Occurring in a Pediatric Patient in the Post-Transplant Setting: Expanding the Spectrum of TRAF7-Mutated Tumors," *Genes, Chromosomes & Cancer* 64, no. 11 (2025): e70092.
20. M. R. Erickson-Johnson, A. R. Seys, C. W. Roth, et al., "Carboxypeptidase M: A Biomarker for the Discrimination of Well-Differentiated Liposarcoma From Lipoma," *Modern Pathology* 22, no. 12 (2009): 1541–1547.
21. P. M. Mazari, K. L. Weber, S. Kim, and P. J. Zhang, "Cytogenetically Confirmed Low-Grade Fibromyxoid Sarcoma Arising From the Tibia," *Human Pathology* 48 (2016): 56–59.
22. M. Parker, K. M. Mohankumar, C. Punchedewa, et al., "C11orf95-RELA Fusions Drive Oncogenic NF- κ B Signaling in Ependymoma," *Nature* 506, no. 7489 (2014): 451–455.
23. D. Figarella-Branger, E. Lechapt-Zalcman, E. Tabouret, et al., "Supratentorial Clear Cell Ependymomas With Branching Capillaries Demonstrate Characteristic Clinicopathological Features and Pathological Activation of Nuclear Factor-kappaB Signaling," *Neuro-Oncology* 18, no. 7 (2016): 919–927.
24. A. Orock, J. A. Zuccato, K. Phan, et al., "TRAF7 in Signaling and Disease: Emerging Mechanisms and Clinical Implications," *Molecular Medicine* 32, no. 1 (2025): 4.